J Fluoresc (2006) 16:595–609
DOI 10.1007/s10895-006-0081-0

ORIGINAL PAPER

Quenchers Induce Wavelength Dependence on Protein Fluorescence Lifetimes

Søren Klitgaard · M. T. Neves-Petersen · S. B. Petersen

Received: 1 December 2005 / Accepted: 6 February 2006 / Published online: 23 June 2006

Abstract We have analysed the picosecond resolved fluorescence emission decay of horseradish peroxidase A2 and of HEW lysozyme acquired with a streak camera. Analyses of the fluorescence decay data of both proteins revealed that the dynamics of the decay is dependent on the emission wavelength. Our data strongly indicates that resonance energy transfer occurring between aromatic residues and different protein fluorescence quencher groups, and the nature of the quencher groups, are the causes of the observed wavelength dependent mean lifetime distribution. Using the global analysis data to calculate the fluorescence mean lifetime at each wavelength revealed that for lysozyme, the mean fluorescence lifetime increased with observation wavelength, whereas the opposite was the case for peroxidase. Both proteins contain strong fluorescence quencher groups located in close spatial proximity to the protein's aromatic residues. Lysozyme contains disulfide bridges as the main fluorescence quencher whereas peroxidase contains a heme group. Both for lysozyme and horseradish peroxidase there is a clear correlation between the observed fluorescence mean lifetime of the protein at a particular emission wavelength and the respective quencher's extinction coefficient at the respective wavelength. Furthermore, our study also reports a comparison of the analyses of the fluorescence data done with three different methods. Analyses of the fluorescence decay at 10 different fluorescence emission wavelengths revealed significant differences in both fluorescence lifetimes and the pre-exponential factor distributions. Such values differed from the values recovered from the integrated decay curves and from global analyse.

Keywords Fluorescence emission lifetimes · Protein fluorescence quenchers · Fluorescence emission wavelength · Peroxidase · Lysozyme · Heme group · Disulfide bridge

S. Klitgaard · M. T. Neves-Petersen · S. B. Petersen (✉)
NanoBiotechnology Group, Department of Physics and Nanotechnology, Aalborg University,
Skjernvej 4C, Aalborg, Denmark
e-mail: sp@nanobio.aau.dk

Introduction

Fluorescence spectroscopy is a powerful, sensitive tool able to provide information on protein dynamic processes, such as intermolecular interactions, solvent effects, protein folding and stability, energy transfer and quenching [1, 2]. One key biophysical parameter that will provide insight into the dynamics of such processes is the fluorescence emission lifetime. Classically, fluorescence emission results from a cascade of relaxation steps leading to progressively lower vibrational states in the first electronic (S_1) excited state, followed by electronic relaxation to various vibrational states in the ground state (S_0). Relaxation from S1's lowest vibrational level to different vibrational levels in the ground state is the cause for the different wavelengths emitted by the molecule.

Typically, time-resolved fluorescence emission spectra are recorded and the fluorescence lifetime recovered at a particular wavelength. This approach does not address the fact that the dynamics of relaxation might be different at different emission wavelengths. Since electronic and vibrational relaxation from the molecule's excited state(s) is dependent on the presence of other groups in the molecule and on the presence of other molecules surrounding the excited molecule, it is expected that the analyses of the dynamics of

fluorescence emission at all emission wavelengths will give us further knowledge on the possible processes that lead to relaxation. For example, tryptophan fluorescence emission (both fluorescence emission maximum and fluorescence emission lifetimes) are used to infer knowledge about the local immediate surroundings of the fluorophore, such as its dielectric constant. It has been known for more than 30 years that the protein fluorescence emission lifetime can depend on the observation wavelength, where the fluorescence mean lifetime typically is reported to increase with observation wavelength [3, 4]. Possible origins of such spectral dependency are reviewed by Lakowicz [5] and Demchenko [6], and they include solvent relaxation, red-edge excitation, viscous media, and oxygen quenching. Protein structures are dynamic entities and the aromatic residues are allowed to explore different conformational landscapes (rotamers). This will influence the dynamics of relaxation of the different amino acids, as shown by Pan and Barkley [7] who reported how tryptophan rotamers display lifetime heterogeneity due to different orientation of the indole relative to the peptide bond, thus changing the quenching efficiency of the carbonyl. The heterogeneity of ground state species (e.g. different conformers, or otherwise different environment) will lead to different relaxation dynamics after photoexcitation. Furthermore, simulations to predict fluorescence quantum yields of tryptophan in proteins by Callis and Liu [8] show the effect of the proximity of charged residues to tryptophan on the tryptophan's fluorescence lifetime and quantum yield. The authors addressed how light-induced electron transfer from tryptophan to a nearby acceptor, which quenches fluorescence, would be either promoted or reduced by vicinal charged groups. Promotion or reduction depends on whether the charge is positive or negative and whether the charge was closer to tryptophan or the electron acceptor. This demonstrates the importance of having insight into photoinduced reaction mechanisms in proteins. Such knowledge builds the foundations for the establishment of correlations attempting to explain the effect of protein electrostatic interactions on the dynamics of fluorescence emission of aromatic residues.

The presence of quenchers is known to change the protein's fluorescence emission lifetime(s) [2, 9–13]. Intrinsic fluorescence quenchers of aromatic residues include disulfide bonds, thiols, carbonyls, tyrosines, lysines, protonated histidines, glutamines, asparagines, glutamic and aspartic acids, and prosthetic groups such as heme [10, 12, 14]. Disulphide bridges and heme groups are known to be among the best protein intrinsic quenchers. Quenching of tryptophan by, e.g. cystines has been reported to happen by electron transfer from the excited state tryptophan to the quencher, and tryptophan is known to eject electrons upon ultraviolet irradiation [15–17]. Extrinsic quenchers such as acrylamide, hydrogen peroxide, cupric ions, chlorinated compounds, and oxygen are also known to be effective fluorescence quenchers [2]. Förster theory can be used to describe quenching, where excited state energy can be transferred from a donor to an acceptor molecule in a radiationless process. The efficiency of the energy transfer depends on the magnitude of the integral overlap between the donor's emission spectrum and the acceptor's absorption spectrum. Both of these quantities are wavelength dependent [18–20]. Energy transfer is highly dependent on the distance between donor and acceptor and on the relative orientation of the dipole moments of the donor and acceptor.

The aim of the present work is to investigate the wavelength-dependence of the fluorescence emission lifetimes in two model proteins, lysozyme and horseradish peroxidase, and to correlate the observed dependence with the presence of endogenous quenchers and their ability to quench differently different parts of the emission spectrum. Our data strongly indicates that resonance energy transfer occurring between aromatic residues and protein fluorescence quencher groups is the cause of the observed wavelength dependent mean lifetime distribution. These two proteins are therefore good candidates to study endogenous quencher effects on the dynamics of the proteins fluorescence emission, since both have strong endogenous fluorescence quenchers in close spatial proximity to their aromatic residues. In order to record simultaneously time and wavelength resolved fluorescence emission spectra, we have made use of streak camera technology. Furthermore, streak cameras provide picosecond time resolution, fast instrument response when compared to multi-channel plate photo-multiplier tubes, and single-photon counting capabilities [21, 22]. This makes streak cameras the ideal technology to study dynamics of protein fluorescence decay at all emitted wavelengths, providing a complete picture of the fast dynamics of the emission decay in one single experiment. Other advantages include reduced photobleaching, reduced experimental time, and that all emission traces have been acquired under the same experimental conditions.

Fluorescence emission lifetime(s) can be recovered by a number of different methods [23–26]. In this study lifetimes have been recovered from the experimental data using three different analysis strategies: (1) upon analyses of selected individual emission wavelengths representative of the whole fluorescence emission band, (2) upon fitting the integrated emission curves, and (3) upon applying global fitting to the datasets. The fluorescence lifetimes recovered using the above mentioned different analysis strategies shines new light into the role of intrinsic protein fluorescence quenchers on the protein's resulting fluorescence lifetime(s). Furthermore, this study alerts the reader to the importance of

the choice of method used to recover fluorescence lifetimes in proteins.

Experimental

Preparation of protein solutions for streak camera investigations

84.6 μM Horseradish peroxidase 5 (Biozyme Laboratories, HRP5, $M_w = 31{,}899$ Da) solutions were prepared in 25 mM acetate buffer, pH 4 and in 25 mM Tris buffer pH 7. 1 mM Lysozyme (Sigma L7651, $M_w = 14{,}300$ Da) was prepared in 25 mM acetate buffer pH 4 and in 25 mM citrate buffer pH 6.

Preparation of solutions for absorbance spectroscopy

Individual solutions of 1.75 mM L-Tyrosine (Sigma, T8909, $\varepsilon_{280\ nm} = 1490\ M^{-1}\ cm^{-1}$), 38.4 mM L-Tryptophan (Sigma, T8659, $\varepsilon_{280\ nm} = 5500\ M^{-1}\ cm^{-1}$), 530 μM lysozyme (Sigma, L7651, $\varepsilon_{280\ nm} = 37970\ M^{-1}\ cm^{-1}$), 4.4 mM trans-1,2-dithiane-4,5-diol (oxidized DTT, Sigma, D3511, $\varepsilon_{310\ nm} = 110\ M^{-1}\ cm^{-1}$) were prepared in MilliQ water. Absorbance spectroscopy on HRPA2 was carried out on the solution prepared for streak camera experiments.

Absorbance spectroscopy

Samples' UV–Vis absorbance was measured in a 1 cm quartz cuvette on a Thermo Electron Corporation UV1 spectrophotometer. To reveal the eventual disulfide bridge contribution to lysozyme's extinction coefficient as a function of wavelength, lysozyme, Trp, and Tyr absorption data were acquired. Afterwards, the contribution from lysozyme's 6 tryptophan and the three tyrosine residues to lysozyme absorption data were subtracted. In order to further investigate disulfide absorption, oxidized DTT and DMDS (dimethyldisulphide) was chosen as model compounds. DMDS absorption cross-section (σ, units of cm^2 per molecule) data were recovered from the work of Hearn *et al.* [27] and converted into extinction coefficient (units of $M^{-1}\ cm^{-1}$) data, according to Smith [28]

$$2.613 \times 10^{20}\sigma = \varepsilon.$$

Streak camera fluorescence spectroscopy

Time-resolved measurements were performed after excitation by ultra-short laser pulses at 280 nm. The pulses were generated by sending the output of a Spectra-Physics Tsunami laser (<100 fs pulse duration, 12 nm FWHM, 80 MHz repetition rate, $\lambda = 840$ nm, Tsunami 3960, Spectra Physics, Mountain View, CA pumped by a high power (5 W at 532 nm) solid state laser Millennia V, Spectra Physics) through a pulse picker, which decreased the pulse repetition rate to 8 MHz. The fundamental pulse was mixed with its second harmonic (420 nm) in a frequency doubler/tripler (GWU; Spectra Physics) to generate 280 nm light pulses. The power at 280 nm was 0.3 mW.

Fluorescence emission was collected perpendicularly to the excitation beam through an input slit (100 μm) of a spectrograph (Oriel, MS257) with a grating blazed at 300 nm with 150 lines/mm (for lysozyme) and a grating blazed at 400 nm with 400 lines/mm (for peroxidase), after which it was focused into the slit of the input optics (100 μm slit) of the streak camera (Optronis, GmbH). Data were acquired for 1.8 ns with 2.6 ps resolution.

Data analysis

The fluorescence decay data were analysed with three different approaches, as explained in the text below.

The fluorescence intensity decays were fitted to an exponential model (Eq. 1) in OriginPro (OriginLab Corp.) using the Levenberg-Marquardt routine. The quality of the fit, evaluated by the χ^2-value and the residual plots, was used to decide, whether a single or a double exponential model was appropriate.

$$I(t) = \sum \alpha_i \exp\left(\frac{-t}{\tau_i}\right) \tag{1}$$

Where α is the pre-exponential factor and τ is the lifetime of the species.

'Single wavelength' decay curves

In the second approach the fitting procedure was performed for 10 individual wavelength traces within the peak in the interval from 310 to 355 nm.

Integrated decay curves

The integrated decay curves were constructed as summation of all wavelength traces in one streak camera image. Each integrated decay curve was then used for fitting to Eq. (1).

Global analysis decays

In this third approach the same 10 wavelength traces as for the single wavelength decay analysis were fitted using global

analysis. The decay was assumed to be characterised by two lifetimes based on the findings in the two other fitting approaches and on the χ^2-values obtained by applying one, two, and three lifetimes in the fitting.
For all fittings the following constraints were made:

$$\alpha_i,\ \tau_i > 0$$

For each dataset in the global analysis fittings the mean lifetime was calculated, according to Neves-Petersen *et al.* [12] as

$$\langle \tau \rangle = \sum_i f_i\, \tau_i$$

where f_i is the fractional intensity calculated as

$$f_i = \frac{\alpha_i\, \tau_i}{\sum_j \alpha_j\, \tau_j}$$

Results

In Fig. 1A and C can be observed the two- and three-dimensional wavelength-resolved fluorescence decays of HRPA2 after 280 nm excitation. In Fig. 1B and D are displayed the wavelength-resolved fluorescence emission of lysozyme after 280 nm excitation. The colour coded emission intensities spectra can be clearly seen in the 3-dimensional plots. The emission decay of HRPA2 is characterized by a very fast initial fluorescence decay that can clearly be seen in Fig. 1A and C. Figure 1B shows clearly that the fluorescence decay of lysozyme is longer lived than what is observed for the HRPA2 sample. Fluorescence decay analyses at different wavelengths revealed that the fluorescence lifetime and/or the pre-exponential factors associated with the fluorescence lifetimes depend on the wavelength at which the analyses was done and on the methodology used to fit the data (global fit, single wavelength and integrated curve analyses).

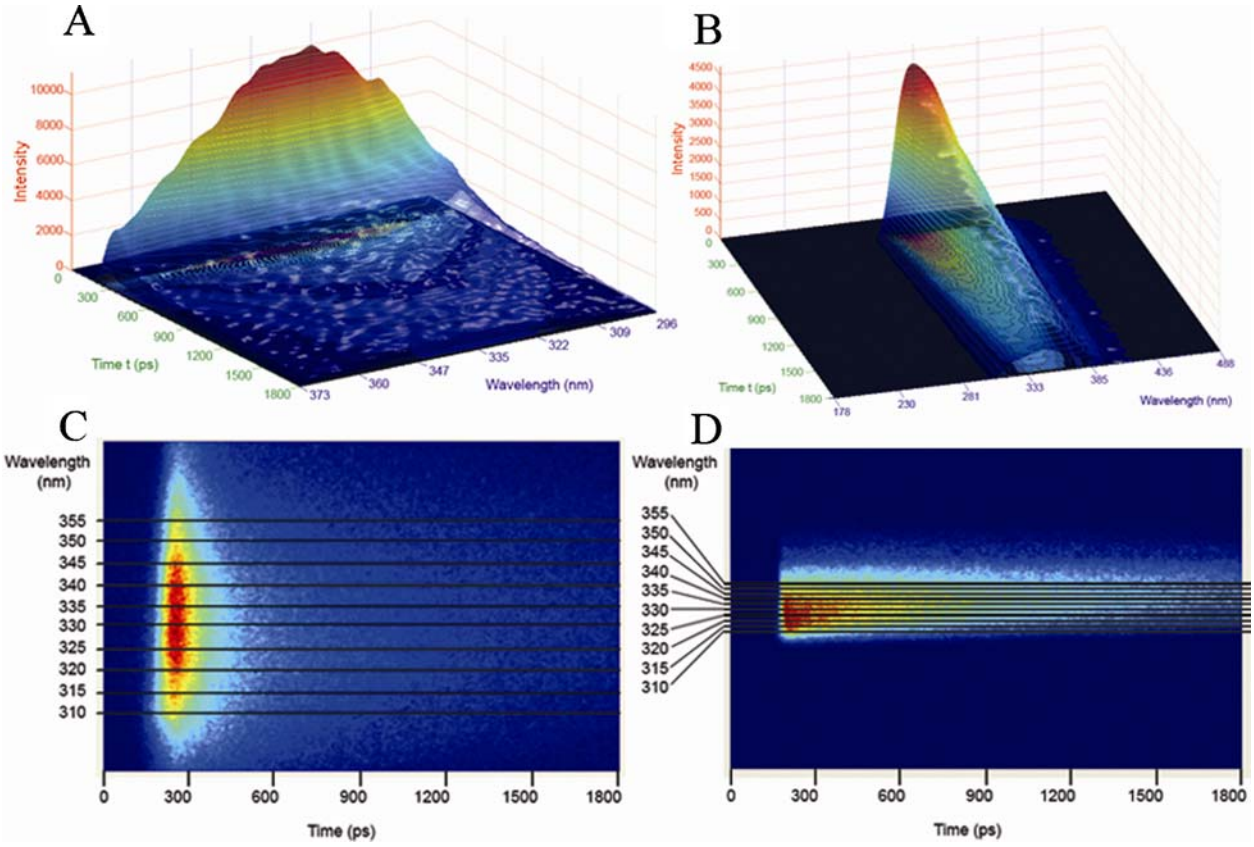

Fig. 1 Three-dimensional streak images displaying the fluorescence emission intensities of HRPA2 (A) and lysozyme (B) at pH 4, after excitation at 280 nm. The colours represents the different intensities, where red is the most intense. Two-dimensional representation of the fluorescence emission intensities of HRPA2 (C) and lysozyme (D) at pH 4, after excitation at 280 nm, where the analysed wavelengths are marked

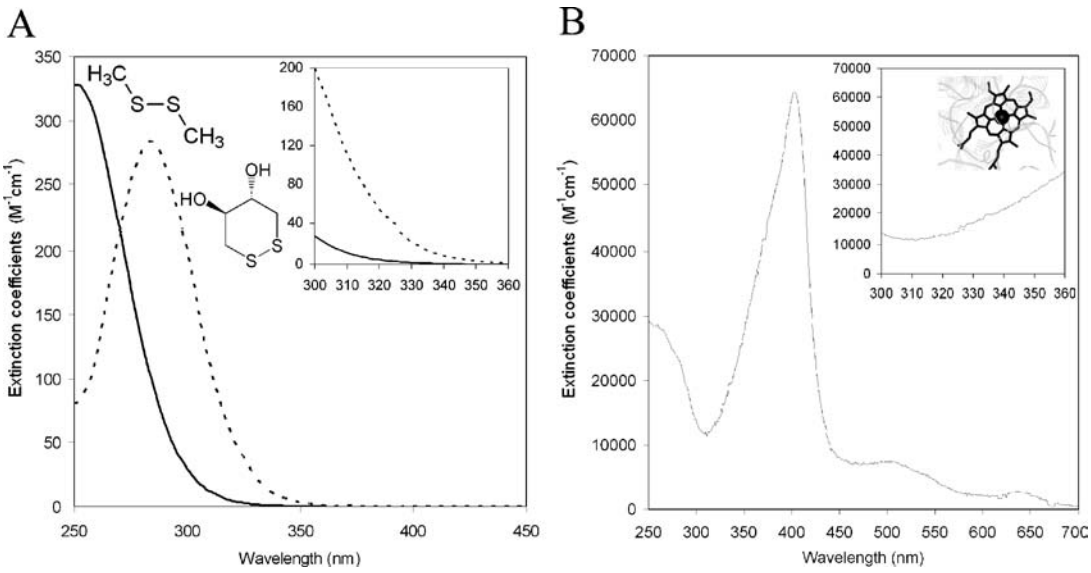

Fig. 2 (A) Absorption spectrum of the oxidised DTT (*punctured line*) and DMDS (*solid line*) used as a model for cystine absorption. In the figure's inset figure is displayed the spectral region where the protein fluorescence emission is monitored. It can be observed that the extinction coefficient decreasing with increasing wavelength. The structure of oxidised DTT (*cyclic structure*) and DMDS are shown. (B) Absorption spectrum of horseradish peroxidase where the distinctive Soret band peaking at 405 nm can be observed. This band is due to the presence of a prosthetic heme-group in HRPA2. In the inset the spectral region is displayed, where the protein fluorescence emission is monitored. It can be observed that the extinction coefficient is increasing with increasing wavelength. The structure of heme within a peroxidase is shown in upper right corner

Absorption data

To investigate spectral effects of intrinsic absorbers in the two proteins two strategies were chosen. For lysozyme it was necessary to use a non-protein disulfide, trans-4,5-dihydroxy-1,2-dithiane (oxidized DTT) to model the intrinsic protein disulfide absorption (Fig. 2A). A constant decrease in absorption intensity is observed with increasing wavelength between 300 and 360 nm (see figures, insert).

In Fig. 2B the absorption spectrum of HRPA2 is displayed, where the characteristic heme absorption with a distinct peak around 405 nm can be observed. The figure's insert highlights the absorption intensity in the spectral region where fluorescence emission has been recorded, from 300 to 360 nm. The absorption is seen to increase from 310 nm to higher wavelengths.

In order to investigate the absorption by disulfide bridges, oxidized DTT and DMDS were chosen as model compounds. Cystine absorption spectrum is extremely sensitive to the dihedral angle. Oxidized DTT dihedral angles were found to be $\pm\chi_1 \sim 66^\circ$, $\pm\chi_2 \sim -61^\circ$, and χ_3 of $\sim 59^\circ$ (CS ChemDraw 3D). It is a fact that such combination of three values for the dihedral angles is not the most commonly seen in proteins [29]. However, we have not run any molecular dynamics simulation at this time. Disulfide absorption in virtually all proteins is believed to be more similar to dimethyldisulfide (DMDS) than to oxidized DTT. The extinction coefficient of oxidized DTT and DMDS above 310 nm (wavelength range that overlaps the protein's fluorescence emission range) are displayed in Figs. 2A and 10. It can be observed that both oxidized DTT and DMDS absorb at wavelengths in the blue edge of the fluorescence emission spectra of lysozyme and that DMDS has extinction coefficients similar to a Trp residue.

In Fig. 10 are displayed the extinction coefficients of lysozyme, Trp, Tyr, oxidized-DTT, and DMDS from 310 to 360 nm. Lysozyme data after subtraction of the extinction coefficient of all aromatic residues in lysozyme that absorb in that wavelength region (Trp, Tyr) is also displayed.

Global analysis decays

The short-lived (τ_{long}) and a long-lived (τ_{short}) lifetimes distribution recovered by *global fitting* are displayed in Fig. 3. For lysozyme the short lifetime component dominates the decay at the short wavelengths. The fluorescence emission decay of peroxidase differs from lysozyme's decay since the shortest component is the dominant component at all wavelengths at both pH 4 and pH 7. An increase of the magnitude of the pre-exponential factor associated with the short-lived component is observed with increasing emission wavelength. The increase is larger at pH 7 than at pH 4. Figure 4A shows how the mean fluorescence lifetime calculated for lysozyme increases over the wavelengths 310–330 nm towards a plateau at wavelengths longer than 330 nm. The calculated mean lifetime for peroxidase decreased constantly as the observation wavelength increased from 310 to 355 nm (Fig. 4B). Data recovered from global analyses are displayed in Tables 1 (lysozyme) and 2 (peroxidase).

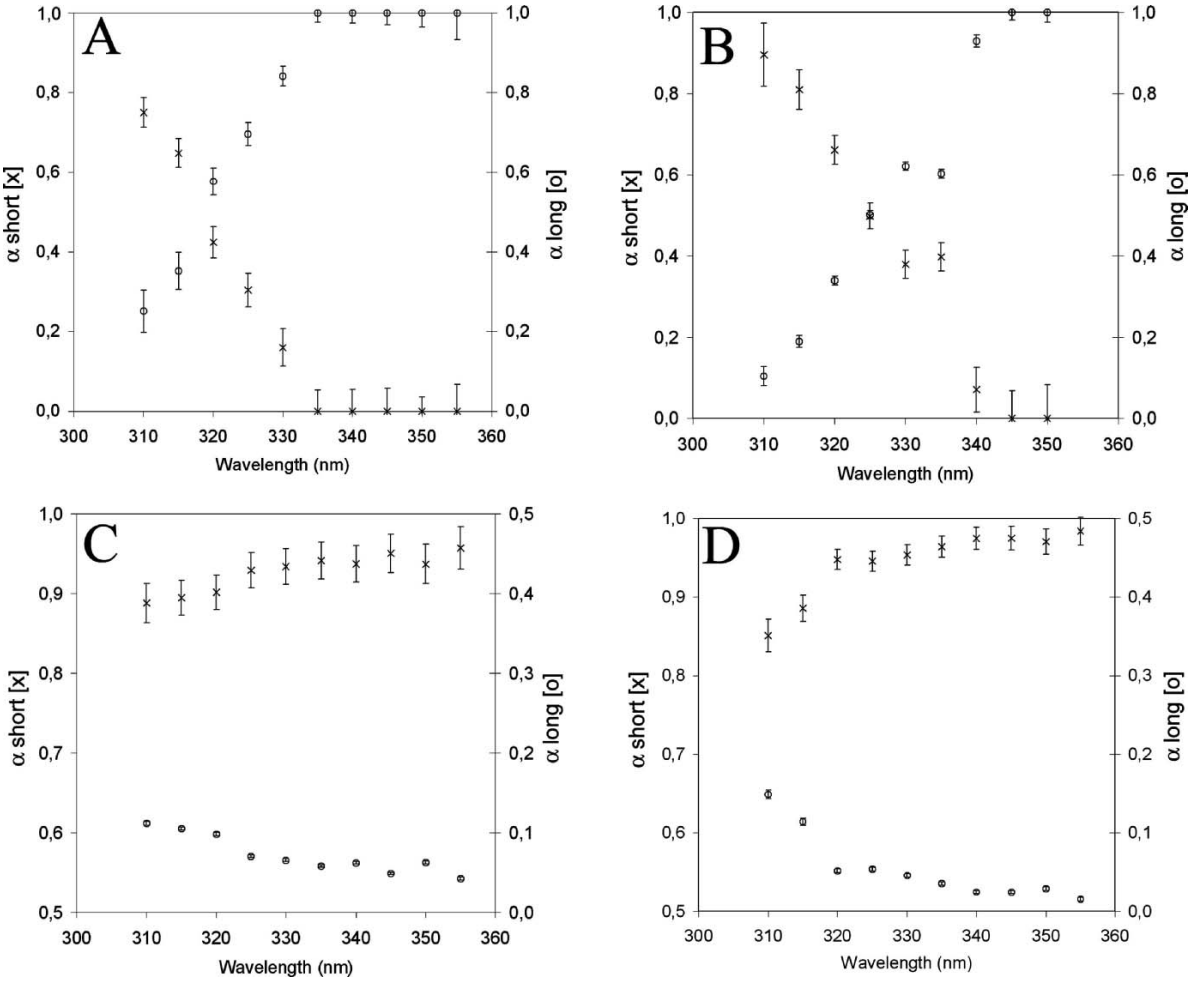

Fig. 3 Plot of the pre-exponential factors of the short lived (×) and the long lived (○) components associated with each fluorescence lifetime, at different observation wavelength obtained by 'global fit analysis': (A) Lysozyme pH 4, (B) lysozyme pH 6, (C) HRPA2 pH 4, (D) HRPA2 pH 7. For lysozyme it can be observed that near the blue edge of the emission the short lifetime component dominates the decay. However, towards the red edge, the long component becomes the dominant component. In the HRPA2 sample the component associated with the short emission lifetime is dominant at all wavelengths and that the fraction of the population preferring the short emission relaxation pathway increases towards the red edge

Table 1 An overview of the lifetimes and pre-exponential factors obtained when global fitting lysozyme datasets

Global analysis,	Lysozyme pH 4			Lysozyme pH 6		
	τ_{short} (331 ± 22 ps)	τ_{long} (1213 ± 110 ps)	$\langle\tau\rangle$ (ps)	τ_{short} (145 ± 8 ps)	τ_{long} (974 ± 47 ps)	$\langle\tau\rangle$ (ps)
λ (nm)	α_{short}	α_{long}		α_{short}	α_{long}	
310	0.75 ± 0.04	0.25 ± 0.05	816	0.90 ± 0.08	0.10 ± 0.02	508
315	0.65 ± 0.04	0.35 ± 0.05	917	0.81 ± 0.04	0.19 ± 0.01	652
320	0.42 ± 0.04	0.58 ± 0.03	1065	0.66 ± 0.04	0.34 ± 0.01	788
325	0.30 ± 0.04	0.70 ± 0.03	1118	0.50 ± 0.03	0.50 ± 0.01	867
330	0.16 ± 0.05	0.84 ± 0.02	1169	0.38 ± 0.03	0.62 ± 0.01	905
335	0.00 ± 0.05	1.00 ± 0.02	1212	0.40 ± 0.04	0.60 ± 0.01	900
340	0.00 ± 0.05	1.00 ± 0.03	1212	0.07 ± 0.06	0.93 ± 0.02	965
345	0.00 ± 0.06	1.00 ± 0.03	1212	0.00 ± 0.07	1.00 ± 0.02	974
350	0.00 ± 0.04	1.00 ± 0.04	1212	0.00 ± 0.08	1.00 ± 0.02	974
355	0.00 ± 0.07	1.00 ± 0.07	1212	–	–	

Note. The data at 355 nm in the pH 6 dataset are omitted from the analysis, since it was not possible to obtain a satisfactory fit to the decay at this wavelength.

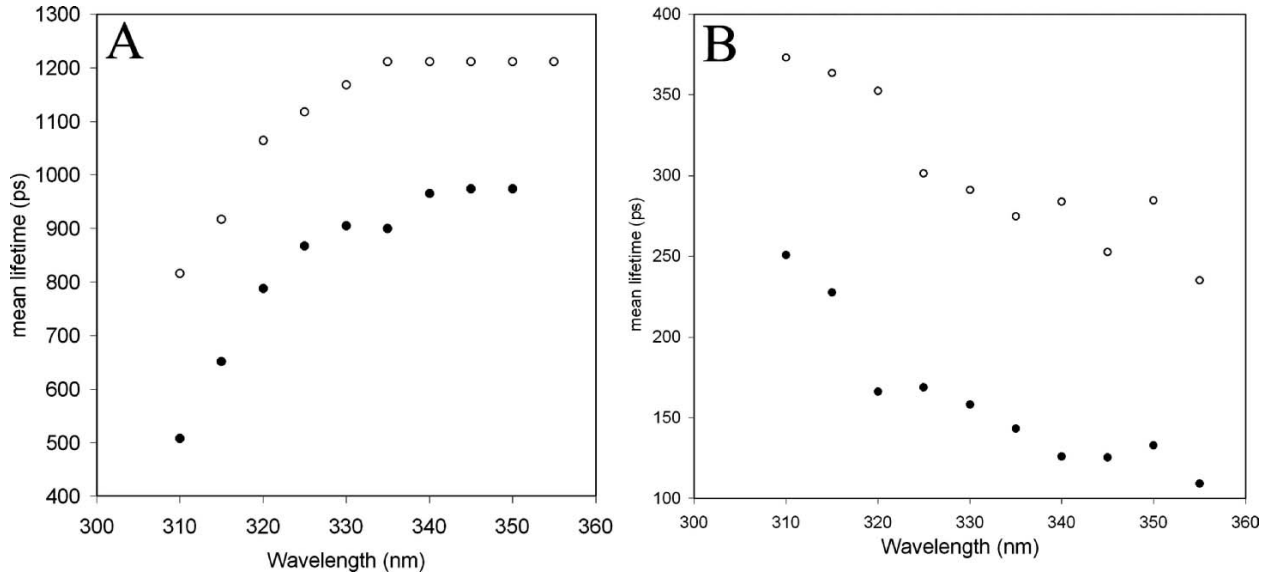

Fig. 4 Mean fluorescence lifetimes calculated after global fit analysis. The fluorescence mean lifetime increased with emission wavelengths for lysozyme (A), both for pH 4 (*open circles*) and for pH 6 (*filled circles*), whereas the mean fluorescence lifetime decreased with emission wavelength for the horseradish peroxidase samples, pH 4 (*open circles*) and pH 7 (*filled circles*)

Figure 5 displays a plot of the mean lifetimes obtained for each protein (Tables 1 and 2, Fig. 4) versus the extinction coefficients of the two strong protein-fluorescence quenchers at the corresponding wavelengths. For lysozyme there is a linear correlation between the extinction coefficient of the disulfide bridge (quencher group) and the calculated fluorescence mean lifetime as a function of fluorescence emission wavelength. For HRP it can be observed that the correlation between the fluorescence mean lifetime and the extinction coefficient of the heme group as a function of wavelength is not linear but biphasic.

'Single wavelength' decays

The analyses of the fluorescence emission decay for lysozyme and for HRPA2 at *individual wavelengths* and different pH values are displayed in Figs. 6 and 7. All lifetimes and pre-exponential factors for lysozyme at pH 4 and 6, and for HRPA2 at pH 4 and 7 are found in Tables 3 and 4, respectively. For lysozyme at pH 4 a double exponential decay was preferred to describe the decay at the lower wavelengths based on χ^2-values obtained using a double exponential model between 63 and 92% of the value obtained using the single exponential model, combined with

Table 2 An overview of the lifetimes and pre-exponential factors obtained when global fitting HRPA2 datasets

	Peroxidase pH 4			Peroxidase pH 6		
Global analysis,	τ_{short} (87 ± 1)	τ_{long} (670 ± 23)	$\langle\tau\rangle$ (ps)	τ_{short} (76 ± 1)	τ_{long} (381 ± 13)	$\langle\tau\rangle$ (ps)
λ (nm)	α_{short}	α_{long}		α_{short}	α_{long}	
310	0.89 ± 0.03	0.11 ± 0.002	373	0.85 ± 0.02	0.15 ± 0.01	251
315	0.90 ± 0.02	0.11 ± 0.002	364	0.89 ± 0.02	0.11 ± 0.004	228
320	0.90 ± 0.02	0.10 ± 0.002	353	0.95 ± 0.01	0.05 ± 0.003	166
325	0.93 ± 0.02	0.07 ± 0.002	302	0.95 ± 0.01	0.05 ± 0.003	169
330	0.93 ± 0.02	0.07 ± 0.002	291	0.95 ± 0.01	0.05 ± 0.002	158
335	0.94 ± 0.02	0.06 ± 0.002	275	0.96 ± 0.01	0.04 ± 0.002	143
340	0.94 ± 0.02	0.06 ± 0.002	284	0.98 ± 0.01	0.03 ± 0.002	126
345	0.95 ± 0.02	0.05 ± 0.002	253	0.98 ± 0.02	0.03 ± 0.002	126
350	0.94 ± 0.03	0.06 ± 0.002	285	0.97 ± 0.02	0.03 ± 0.002	133
355	0.96 ± 0.03	0.04 ± 0.002	235	0.98 ± 0.02	0.02 ± 0.002	109

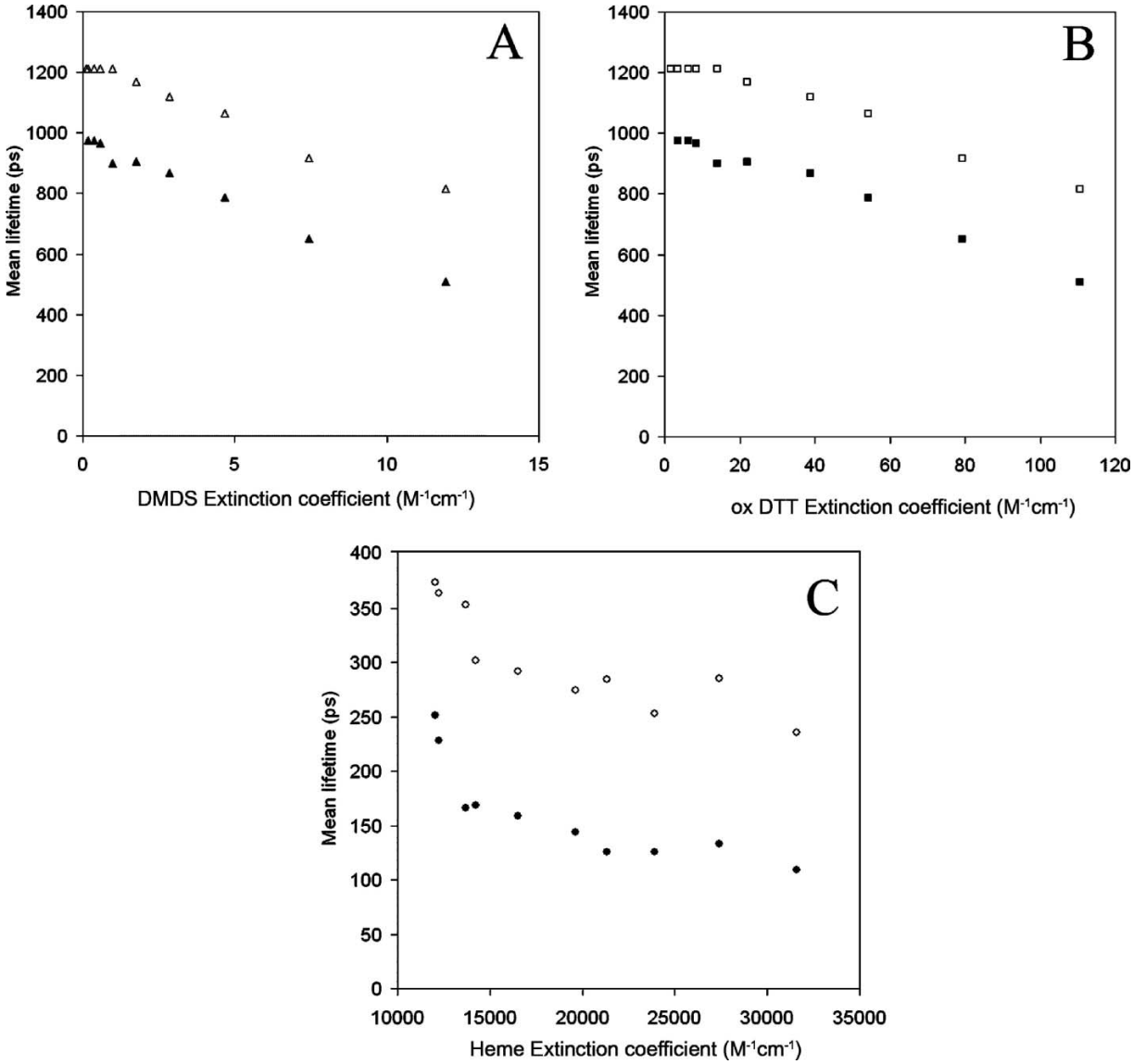

Fig. 5 Plots of the mean lifetime versus the extinction coefficient of a quencher (absorber) at corresponding wavelengths. (A) The mean fluorescence lifetime of lysozyme at pH 4 (*open triangles*) and pH 6 (*filled triangles*) versus the extinction coefficient of DMDS. (B) The mean fluorescence lifetime of lysozyme at pH 4 (*open squares*) and pH 6 (*filled squares*) vs. the extinction coefficient of oxidised DTT. (C) The mean fluorescence lifetime of HRPA2 at pH 4 (*open circles*) and pH 7 (*filled circles*) versus the extinction coefficient of the heme group in HRPA2

the residuals. For wavelengths above 330 nm the decay was best described by a single-exponential decay with lifetimes increasing from 995 ± 40 ps, at 330 nm, to 2041 ± 330 ps, at 355 nm. At pH 6, a double exponential decay gave the best fit from 310 to 335 nm based on χ^2-values values from the double exponential fit between 61 and 85% of the χ^2-values obtained from the single exponential, supported by the residual plots, whereas a single exponential fit was sufficient from 340 to 355 nm. In the 310–335 nm interval the shorter lifetime dominates the decay, with pre-exponential factors starting at 0.82 ± 0.23 at 310 nm and decreasing to 0.47 ± 0.17 at 335 nm. The lifetime of the longer lived relaxation pathway increased with increasing wavelength going from around 400 ps at 310 nm to approximately 1900 ps at 355 nm. The shorter lifetime displays a parabolic curve with a minimum around 325 nm. There are however large errors associated with the pre-exponential factors of the shorter lived species in the fluorescence emission decay of lysozyme at both pH values (Fig. 8A and B).

For HRPA2 at both pH values the fluorescence emission decay was best fitted with a double exponential decay at all

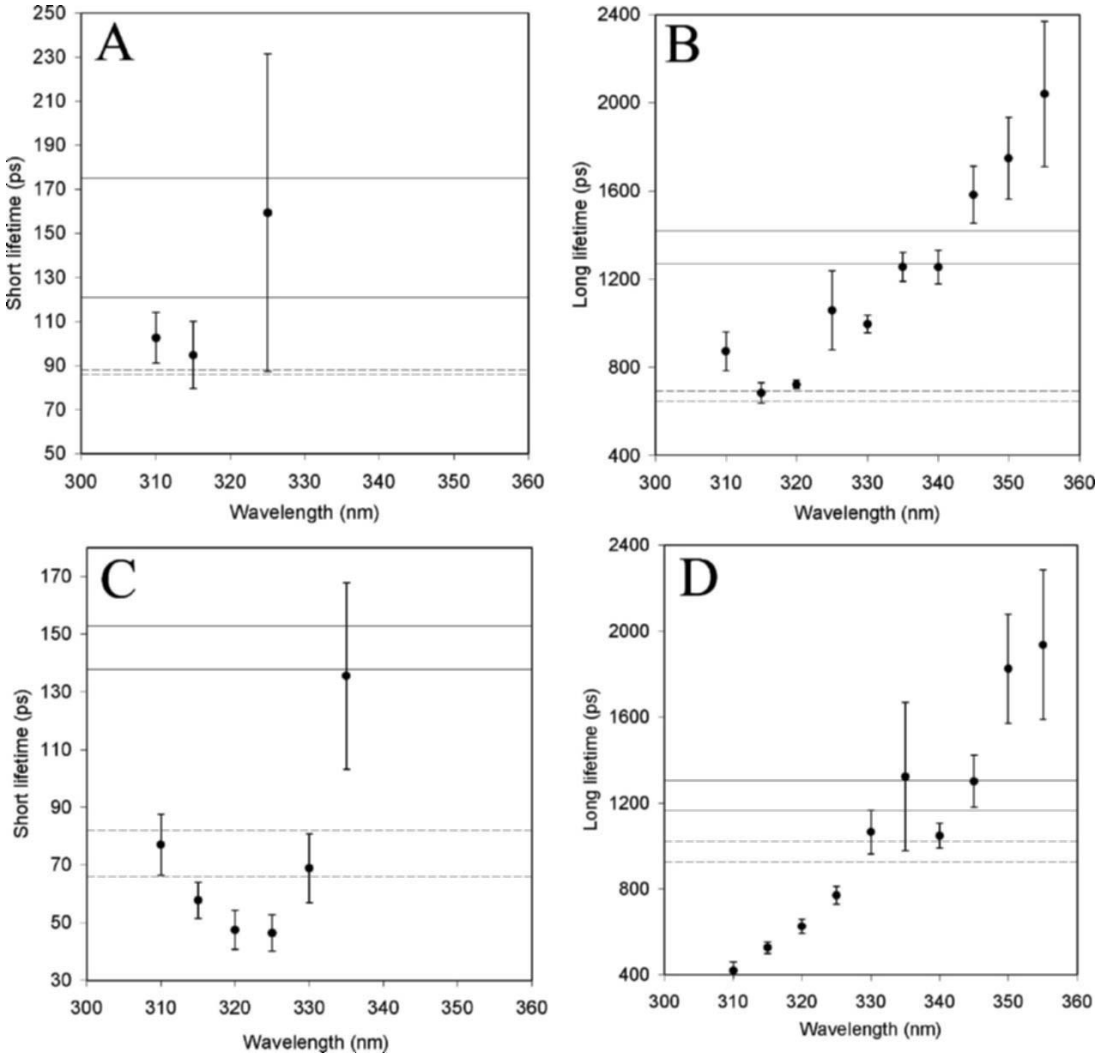

Fig. 6 Comparison of the different fluorescence emission lifetimes recovered upon analysing the experimental data sets for lysozyme with 'single wavelength' fitting routine, global fitting analysis and 'integrated curve' analyses. The single wavelength data are displayed as datapoints, and the horizontal lines represent the lifetime interval, i.e. lifetime with associated error, of the corresponding component obtained when carrying on global fitting analysis of the fluorescence emission data set (*punctured line*) and when fitting the integrated curve emission spectrum (*solid line*). (A) Lysozyme pH 4, short lifetime component, (B) lysozyme pH 4, long lifetime component, (C) lysozyme pH 6, short lifetime component, (D) lysozyme pH 6, long lifetime component

wavelengths with one single exception at 355 nm at pH 7, where a single-exponential model was sufficient to describe the decay. For all fluorescence decay fits for peroxidase at pH 4 the double exponential fit provided a reduction of χ^2-values to 52% or less of the value obtained by fitting using a single exponential. At pH 7 the peroxidase fluorescence emission the χ^2-values obtained by using the double exponential model were between 50 and 85% of the values obtained using a single exponential model, when the double exponential model was preferred. At 355 nm the χ^2-value from the double exponential model fit was 93% of the χ^2-value at the single exponential model fit, and the inspection of the fitting residuals did not suggest preferring a double exponential model. At all wavelengths the short decay component was dominant. At the blue edge of the emission peak the pre-exponential factor of the short component is 0.89 ± 0.08 at pH 4 and 0.87 ± 0.04 at pH 7. At both pH values these pre-exponential factors increase to 0.97 ± 0.08 at pH 4 and 1.00 ± 0.02 at pH 7 as the observation wavelength goes towards the red edge of the peak. At pH 4 both the short and the long lifetimes (Fig. 7A and D) varies with wavelength and there is a minimum at 335 nm (Table 4). Towards the edges of the peak an apparent increase in both lifetimes is observed. The same pattern is not observed at pH 7 (Fig. 7C and D) where the apparent lifetimes fluctuate with the observation wavelengths.

Table 3 An overview of the lifetimes and pre-exponential factors recovered from fitting the single wavelengths one by one in both lysozyme datasets

Single wavelength, λ (nm)	Lysozyme pH 4				Lysozyme pH 6			
	α_{short}	τ_{short}	α_{long}	τ_{long}	α_{short}	τ_{short}	α_{long}	τ_{long}
310	0.64 ± 0.12	103 ± 12	0.36 ± 0.03	873 ± 88	0.82 ± 0.23	77 ± 11	0.18 ± 0.11	420 ± 40
315	0.55 ± 0.19	95 ± 15	0.45 ± 0.03	685 ± 47	0.87 ± 0.29	58 ± 6	0.13 ± 0.03	527 ± 27
320	–	–	1.00 ± 0.01	723 ± 19	0.91 ± 0.48	48 ± 7	0.09 ± 0.02	627 ± 34
325	0.23 ± 0.19	159 ± 72	0.77 ± 0.03	1059 ± 180	0.90 ± 0.48	47 ± 6	0.10 ± 0.01	772 ± 41
330	–	–	1.00 ± 0.01	996 ± 40	0.71 ± 0.39	69 ± 12	0.29 ± 0.02	1066 ± 101
335	–	–	1.00 ± 0.02	1257 ± 66	0.47 ± 0.17	136 ± 32	0.53 ± 0.04	1323 ± 344
340	–	–	1.00 ± 0.02	1255 ± 78	–	–	1.00 ± 0.02	1048 ± 59
345	–	–	1.00 ± 0.04	1583 ± 129	–	–	1.00 ± 0.04	1301 ± 121
350	–	–	1.00 ± 0.06	1749 ± 186	–	–	1.00 ± 0.08	1824 ± 254
355	–	–	1.00 ± 0.10	2041 ± 330	–	–	1.00 ± 0.10	1937 ± 347
Integrated decay	0.22 ± 0.03	148 ± 27	0.78 ± 0.01	1346 ± 75	0.80 ± 0.25	74 ± 8	0.20 ± 0.00	1234 ± 70

Note. Two lifetimes are listed when a bi-exponential decay was necessary to fit the fluorescence decay. When one lifetime was sufficient, there is only one fluorescence lifetime reported. The lifetimes and pre-exponential factors recovered, when fitting the 'integrated curves' of lysozyme are also displayed.

Integrated decay

The integrated fluorescence emission decay curves were best fitted by a double exponential model. For lysozyme the χ^2-values were reduced to 88 and 77% of the χ^2-values obtained by a single exponential fit at pH 4 and pH 6 respectively. Further the residuals supported the double exponential model. For HRPA2 the χ^2-values were reduced to 3 and 14% at pH and pH 7 of the χ^2-values obtained by fitting to the single exponential model. For lysozyme at pH 4 the short lifetime is found to be 148 ± 27 ps ($\alpha_{short} = 0.22 \pm 0.03$) and the long lifetime 1346 ± 75 ps ($\alpha_{long} = 0.78 \pm 0.01$) dominates the decay (Table 3). At pH 6 the decay is faster, where the short lifetime that dominates the decay is 74 ± 8 ps ($\alpha_{short} = 0.80 \pm 0.25$) and the longer lifetime is 1234 ± 70 ps ($\alpha_{long} = 0.20 \pm 0.00$) (Table 3).

For HRPA2 the fluorescence emission lifetimes display the same trend as for lysozyme: both the longer and the shorter lifetime decay faster at the higher pH. (Table 4) The pre-exponential factor associated with the shorter lifetime however is practically the same for both pH values with 0.96 ± 0.1 at pH 4 and 0.97 ± 0.1 at pH 7.

Figure 9 shows the fit of a double exponential decay to the temporal fluorescence emission trace of HRPA2 at pH 4 analysed at a single wavelength, 325 nm. The residuals are plotted below. The χ^2-value of the double exponential fit decreased to 28% of the value obtained by the single exponential fit. A triple exponential fit did not improve the χ^2-value.

Table 4 An overview of the lifetimes and pre-exponential factors recovered from fitting the single wavelengths one by one in both horseradish peroxidase datasets

Single wavelength, λ (nm)	Peroxidase pH 4				Peroxidase pH 7			
	α_{short}	τ_{short}	α_{long}	τ_{long}	α_{short}	τ_{short}	α_{long}	τ_{long}
310	0.89 ± 0.08	97 ± 5	0.11 ± 0.03	1015 ± 167	0.87 ± 0.04	105 ± 7	0.13 ± 0.19	469 ± 79
315	0.87 ± 0.05	128 ± 7	0.13 ± 0.09	1483 ± 561	0.91 ± 0.18	42 ± 3	0.09 ± 0.06	248 ± 10
320	0.93 ± 0.07	100 ± 4	0.11 ± 0.02	1063 ± 187	0.96 ± 0.04	75 ± 2	0.04 ± 0.13	479 ± 74
325	0.94 ± 0.06	87 ± 3	0.07 ± 0.04	732 ± 77	0.97 ± 0.03	90 ± 2	0.03 ± 0.11	769 ± 240
330	0.94 ± 0.07	77 ± 3	0.06 ± 0.05	611 ± 49	0.93 ± 0.05	63 ± 2	0.07 ± 0.13	274 ± 21
335	0.94 ± 0.08	74 ± 3	0.06 ± 0.07	431 ± 28	0.98 ± 0.03	84 ± 2	0.02 ± 0.07	1022 ± 462
340	0.94 ± 0.06	87 ± 3	0.06 ± 0.07	624 ± 65	0.98 ± 0.03	78 ± 1	0.02 ± 0.12	1198 ± 631
345	0.94 ± 0.08	84 ± 4	0.06 ± 0.12	470 ± 56	0.98 ± 0.03	73 ± 2	0.02 ± 0.11	697 ± 192
350	0.93 ± 0.06	101 ± 4	0.07 ± 0.04	1152 ± 325	0.96 ± 0.04	76 ± 3	0.04 ± 0.39	293 ± 66
355	0.97 ± 0.08	75 ± 3	0.03 ± 0.06	775 ± 133	1.00 ± 0.02	84 ± 1	–	–
Integrated decay	0.96 ± 0.01	96 ± 1	0.04 ± 0.00	806 ± 16	0.97 ± 0.01	87 ± 1	0.03 ± 0.00	666 ± 30

Note. Two lifetimes are listed when a bi-exponential decay was necessary to fit the fluorescence decay. When one lifetime was sufficient, there is only one fluorescence lifetime reported. The lifetimes and pre-exponential factors recovered, when fitting the 'integrated curves' of HRPA2 are also displayed.

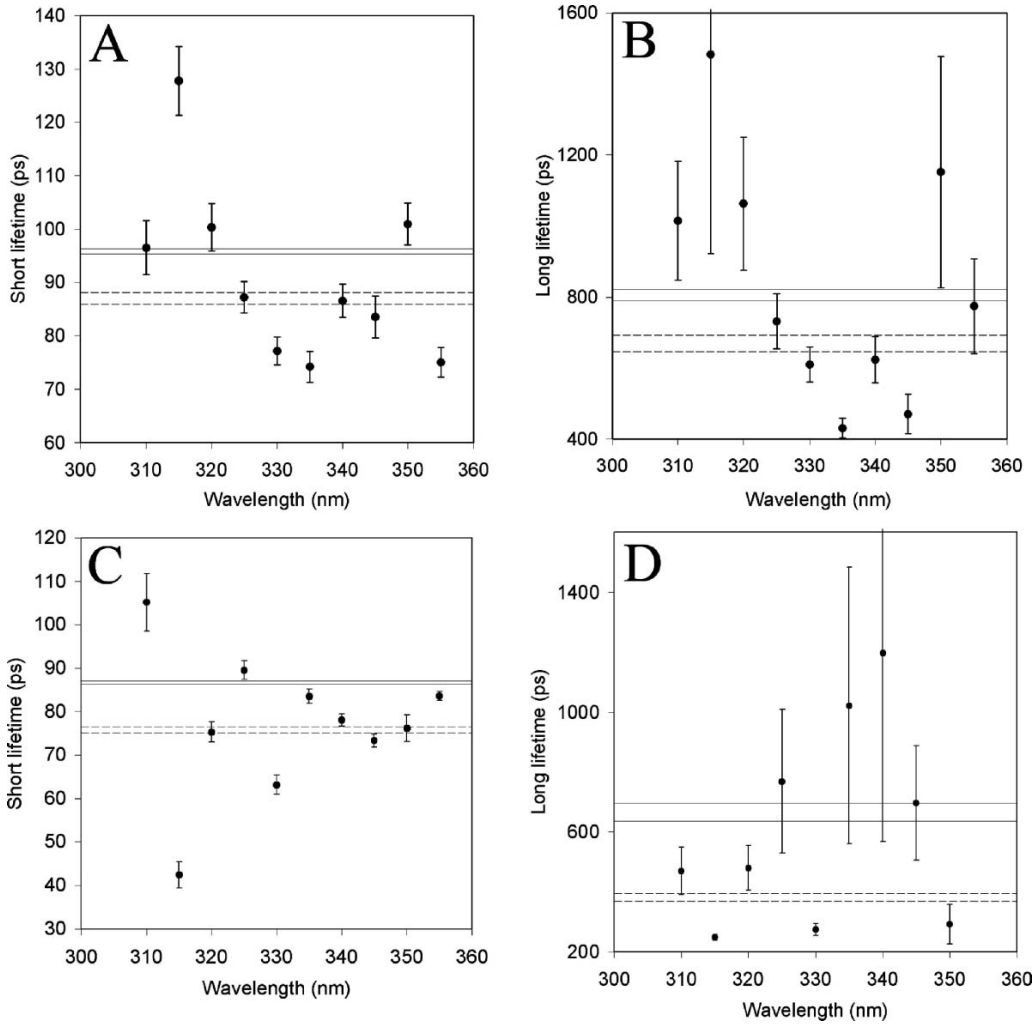

Fig. 7 Comparison of the different fluorescence emission lifetimes recovered upon analysing the experimental data sets for HRPA2 with 'single wavelength' fitting routine, global fitting analysis and 'integrated curve' analyses. The single wavelength data are displayed as datapoints, and the horizontal lines represent the lifetime interval, i.e. lifetime with associated error, of the corresponding component obtained when carrying on global fitting analysis of the fluorescence emission data set (*punctured line*) and when fitting the integrated curve emission spectrum (*solid line*). (A) HRPA2 pH 4, short lifetime component, (B) HRPA2 pH 4, long lifetime component, (C) HRPA2 pH 7, short lifetime component, (D) HRPA2 pH 7 long lifetime component

Discussion

Different methodologies for data analyses

Three different methods used to analyse the fluorescence lifetime decay data have been applied. The advantage of using the integrated decay curve to recover the lifetimes and pre-exponential factors is that the integrated decay curve, by summing up all wavelengths, has a very good signal-to-noise compared to the signal to noise level of the individual traces. Provided that the integrated decay curve retains its exponential decay nature, the calculated decay parameters will have small errors. However, there is no spectral information in the data recovered from the integrated decay curve. When analysing the data at individual wavelength traces it is then possible to observe how lifetimes and pre-exponential factors associated to the fluorescence emission pathways vary with observation wavelength. This methodology is preferred to the integrated decay curve method since it will give us insight into the dynamics of relaxation as a function of emission wavelength. Sometime the errors associated with the data are large, thus blurring eventual wavelength dependent trends regarding both short-lived and long-lived lifetimes, as well as pre-exponential factors. However, with the advent of ever more sensitive detectors, the signal to noise ratio of the collected data will allow for precise data analysis of individual decay curves. This is now feasible, and the present data set documents this claim. Therefore, we can now analyse the individual decay curves with reasonably small errors. In such conditions, single wavelength analysis is a must since

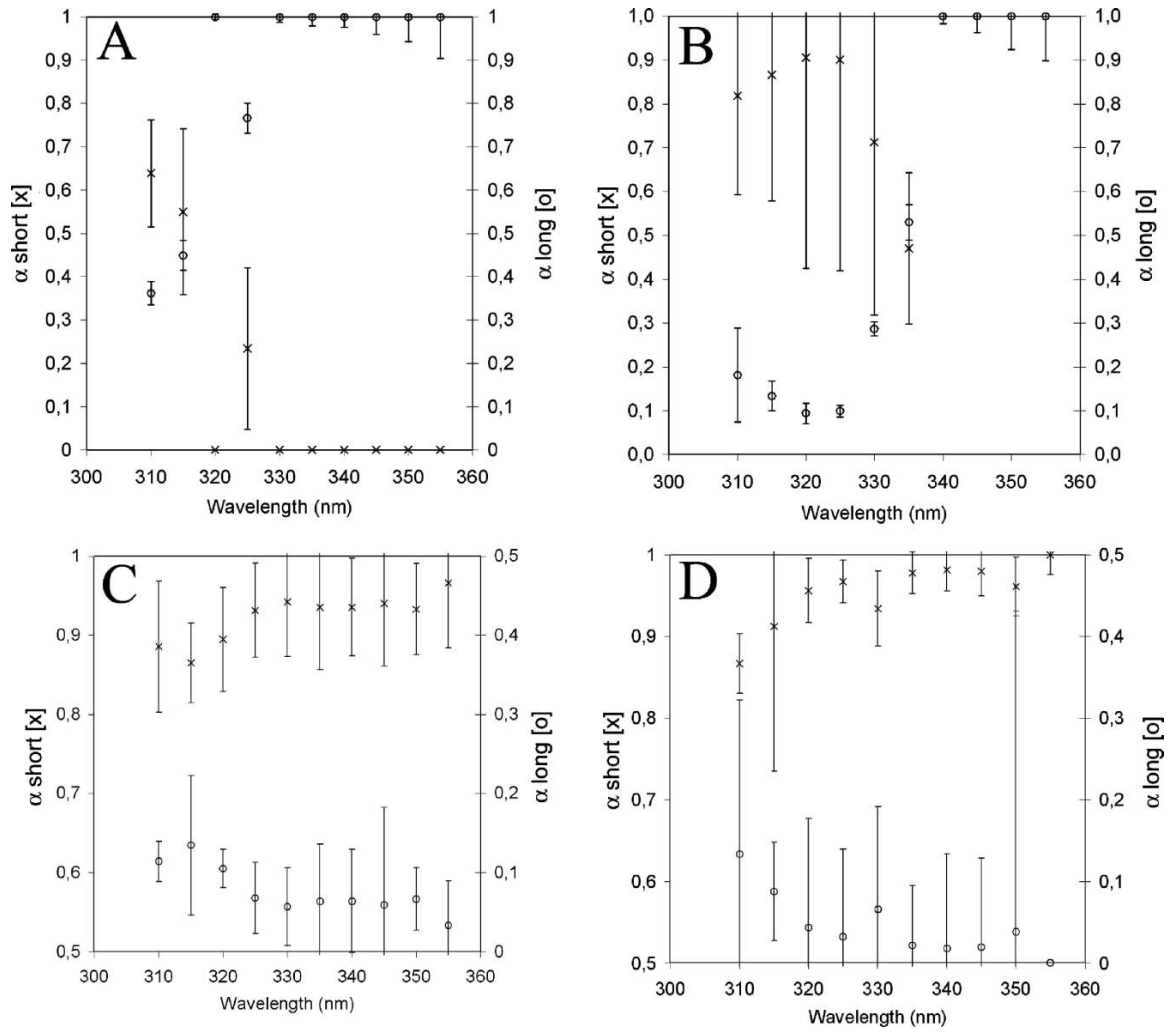

Fig. 8 Plot of the pre-exponential factors of the short lived (×) and the long lived (○) components obtained when fitting the fluorescence emission decays at single wavelengths with a multi-exponential decay model ('single wavelength' fitting routine approach): (A) Lysozyme pH 4, (B) lysozyme pH 6, (C) HRPA2 pH 4, (D) HRPA2 pH 7

it will reveal the dynamics of relaxation as a function of wavelength. This will allow further insight into the causes of such dynamics. Global analysis offers the advantage of better signal to noise ratio of the dataset allowing the recovery of parameters with small associated errors.

Data discussion

A possible origin of the observed multiple fluorescence lifetimes is the different possible rotamers in the ensemble of protein molecules. The different conformations will most likely give rise to different relative orientation between aromatic residues and possible fluorescence quenchers in the molecules, therefore influencing the rate of resonance energy transfer. The observed spectral dependence of the lifetime distribution could also be due to the fact that with 280 nm light we also excite both tryptophan and tyrosine residues. Since these residues can transfer energy among them, this could lead to a wavelength dependent lifetime distribution. Important for the interpretation lysozyme data is to discuss the role of Trp, Tyr and disulphide bridges as protein fluorescence quencher groups. Important to the discussion of horseradish peroxidase data is to additionally discuss the observation that the presence of the heme group in proteins leads to well known changes in the dynamics of fluorescence relaxation, as reported by Kamal and Behere [11] and Carvalho *et al*. [13].

Lysozyme data discussion

The origin of the multiple fluorescence lifetimes in lysozyme is likely due to the presence of 6 tryptophan residues and 3 tyrosine residues. These residues are distributed in different local protein environments (some solvent accessible, other buried), thus having most likely different dynamics of relaxation. The different environments of the 6 Trp residues

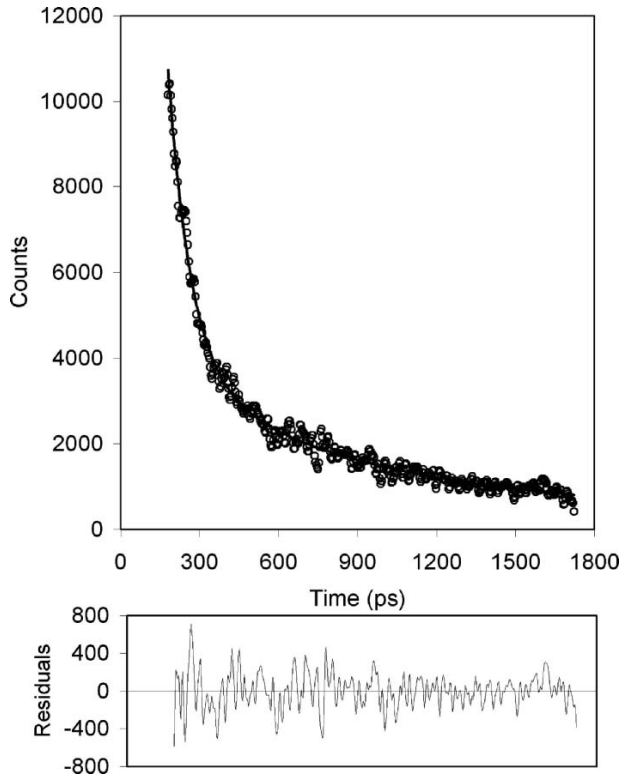

Fig. 9 Fluorescence emission trace of HRPA2 at pH 4 analysed at a single wavelength, 325 nm (*open circles*). The decay is fitted with a two-exponential decay (*line*). The residuals are plotted below

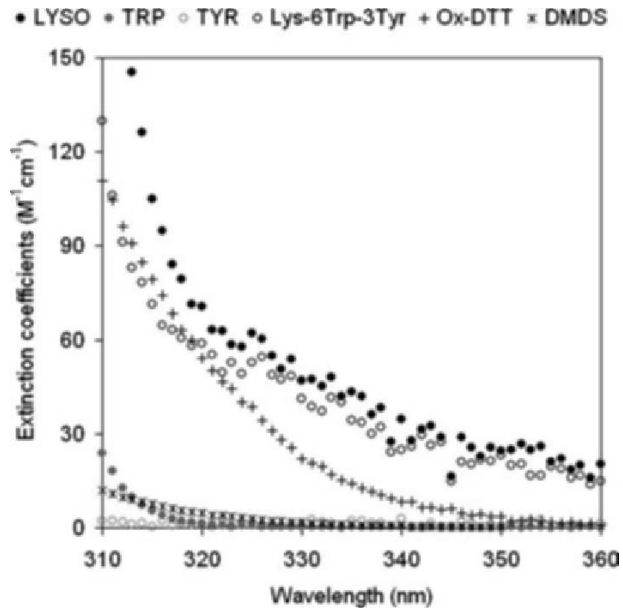

Fig. 10 Extinction coefficients of lysozyme (Lysozyme), tryptophan (Trp), tyrosine (Tyr), and of lysozyme after subtracting the contribution from 6 Trp and 3 Tyr (Lysozyme-6Trp-3Tyr) above 310 nm. The extinction coefficients of two disulfide model compounds, oxidized DTT and dimethyldisulfide, are also displayed above 310 nm (wavelength range that coincides with the protein's fluorescence emission)

could lead to different fluorescence emission spectra, with the possibility of resonance energy transfer from the blue edge of the emission spectra, since it will overlap Trp excitation spectrum. This will contribute to the observed spectral dependence of the average fluorescence lifetime reported for lysozyme. The presence of different Trp rotamers will influence the dynamics of relaxation due to different orientation of the indole relative to the peptide bond, as shown by Pan and Barkley [7]. This will also contribute to the observed spectral dependence. In addition, the 3 tyrosine residues fluoresce at short wavelengths and can transfer their energy to Trp residues, again contributing to the observed effect.

The presence of different rotamers in the ensemble of protein molecules will most likely give rise to different relative orientation between aromatic residues and possible fluorescence quenchers in the molecules, therefore influencing the rate of resonance energy transfer. Disulphide bridges are known to be strong fluorescence quenchers. If their extinction coefficient is larger at the blue edge of protein's fluorescence emission spectra than at the red edge of the emission spectra, then this could contribute to the observed spectral dependence of the mean fluorescence lifetimes reported for lysozyme. As reported in the results section (Figs. 2A and 10) both oxidized DTT and DMDS absorb at wavelengths in the blue edge of the fluorescence emission spectra of lysozyme (above 310 nm). DMDS has extinction coefficients similar to Trp residue while oxidized DTT displays even larger absorbance values (more than 5 times larger). These two compounds contain a disulphide bridge and most likely mimic cystine absorption in the protein molecule. As can also be observed in Fig. 10, after subtracting the contribution of lysozyme's 6 tryptophan and 3 tyrosine residues from lysozyme absorption data, lysozyme is still absorbing above 310 nm. This can not be due to absorption by Trp, Tyr, Phe, His or even carbonyl groups. The only likely groups that will absorb above 310 nm are the 4 disulphide residues in lysozyme. These combined observations suggest that it is likely that light absorption above 310 nm is due to the 4 disulphide bridges in this molecule and that this also will contribute to the observed spectral dependence of the average fluorescence lifetime reported for lysozyme (increase of mean lifetime from the blue to the red edge of emission).

Horseradish peroxidase A2 data discussion

Horseradish peroxidase has 1 Trp, 2 Tyr and 8 cysteine residues, assumed to form 4 disulphide bridges due to its homology to HRPA1 (1ATJ.pdb) [29], and a heme group, known to be an extremely good quencher of protein fluorescence. HRPA2 displays an opposite spectral dependence of the average mean lifetime to the one observed in lysozyme, since a decrease of the fluorescence mean lifetime is observed from the blue to the red edge of emission spectrum.

In order to gain insight into the causes of the observed spectral dependence of the average mean lifetime in HRPA2, we need to investigate the role of the heme group. The extinction coefficient of the Heme group increases from 310 to 360 nm, the wavelength range that overlaps the protein's emission spectrum, Furthermore, the heme extinction coefficient is 1–4 orders of magnitude larger (from 310 to 350 nm) than the extinction coefficients of other absorbing species (Trp, Tyr, cystine) in the observed spectral range. Heme absorption from 310 to 360 nm is therefore the stronger likely cause explaining the spectral dependence of mean fluorescence lifetimes observed for HRPA2, overruling all other possible effects reported for lysozyme that might affect the spectral dependency of a protein's emission.

Carvalho *et al.*'s [13] analysis of the fluorescence lifetime distribution of the heme depleted horseradish peroxidase reveals the absence of the short lifetime component, resulting in an increase of the mean fluorescence lifetime for the heme depleted enzyme. They report a mean fluorescence lifetime of 0.474 and of 2.368 ps for the holo- and apo-enzymes, respectively. The dynamics of relaxation of the holo-protein was dominated by an extremely short lifetime of 55 ps ($\alpha_1 = 0.92$). This short lifetime was not observed in the heme depleted protein. The very fast fluorescence lifetime ($\sim$76 ps, Table 2) observed during our study for horseradish peroxidase A2 is most likely due the presence of the very strong protein fluorescence quencher, the heme group. The heme is located in close spatial proximity to the single tryptophan residue in horseradish peroxidase A2, thus providing a strong quenching pathway. We assume that the presence of such strong fluorescence quencher could be the dominant cause of the observed spectral dependence of the recovered mean lifetimes, since the heme group will quench more strongly the red edge that the blue edge of the emission spectra of aromatic residues.

The two tyrosine residues in HRPA2 may be contributing to the slower component at short wavelengths and the Trp, which emits at longer wavelengths (and is therefore more efficiently quenched by the heme) can be responsible for the fast component. Protein excitation at 295–297 nm, that selectively excites Trp residues, could attempt to separate the role of Trp and Tyr residues to the observed HRPA2 relaxation dynamics. Studies by Kamal and Behere [11] and Carvalho *et al.* [13] shows, that at least three fluorescence lifetimes can be resolved in both the holo- and the apo-forms of the related peroxidases HRPC, HRPA1, and seed coat soybean peroxidase upon 295–297 nm excitation. The holo-enzymes have a faster decay channel than the apo-forms. Since the apo form of the enzymes displays three fluorescence lifetimes, it points at that the single tryptophan in the peroxidases can populate different conformational states that provides different decay routes.

Due to the dynamic behaviour of proteins, the single Trp residue in HRPA2 will populate the conformational space that is allowed to, being this way present as different rotamers in the ensemble of protein molecules. This indeed will mean that the relative orientation between Trp and Heme will be different from molecule to molecule, and in the same molecule due to likely molecular conformational changes. This will affect the efficiency of resonance energy transfer (RET) from Trp to Heme. It is also possible that there are two or more conformations of the Trp, one with a poor orientation for RET. These different conformations will contribute to different fluorescence lifetimes for HRPA2.

Final discussion of correlated data

We have reported a direct correlation between the spectral changes in a protein's fluorescence emission mean lifetime and extinction coefficients of quenchers in the spatial and spectral vicinity of tryptophan residues, both in horseradish peroxidase and lysozyme. The correlation highlights the role of the quencher on the dynamics of protein fluorescence decay. The observed data indicates that the protein aromatic residues act as donors that transfer their excited state energy to possible protein quenchers such as disulphide bridges, heme group, the aromatic residues themselves that act as acceptors.

For both lysozyme and peroxidase it should be noticed that over the wavelengths reported there is an inverse trend between the fluorescence emission mean lifetime determined by global analysis and the extinction coefficients of possible main acceptors in the protein. Regarding lysozyme, there is a linear correlation between the fluorescence emission mean lifetime and the extinction coefficient of disulfide bridges as a function of wavelength, as displayed in Fig. 5 (graphs A, B). This shows that the ability of a disulfide bridge to quench protein fluorescence will influence directly the speed of fluorescent relaxation from lysozyme in the excited state. Neves-Petersen *et al.* [30] showed that disulfide bridges are preferred structural neighbours of aromatic residues. If this observation is combined with the correlation between mean fluorescence lifetime of lysozyme and disulfide extinction coefficient this might explain why mean fluorescence lifetime of proteins often is reported to increase with observation wavelength [5, 6]. A very large proportion of proteins contain one or more disulphide bridges. Thus the reported red-shift is consistent with disulphide containing proteins. Peroxidase fluorescence emission mean lifetime displayed versus the extinction coefficient of the protein's heme group (Soret band) reveals a biphasic correlation. At the lower extinction coefficients a steep decline over a few points is observed, and a less steep decline is noticed at higher extinction coefficients. No explanation is presented at the moment.

Conclusion

Our work provides evidence that protein strong fluorescence quencher groups such as disulphide bridges and heme groups contribute to the spectral dependence of the average mean lifetime observed in lysozyme and horseradish peroxidase. Further, it should be noted that the methodology used for analysis of fluorescence emission decays have a large influence on the amplitudes of the lifetimes and pre-exponential factors that are recovered.

Acknowledgements M.T.N.-P. acknowledges the support from Novi Invest and Licfond and from the Danish Research Agency, Novo Nordisk A/S, Novozymes A/S.

References

1. Bright FV, Munson CA (2003) Time-resolved fluorescence spectroscopy for illuminating complex systems. Anal Chim Acta 500:71–104
2. Lakowicz JR (1999) Principles of fluorescence spectroscopy, 2nd edn. Kluwer Academic/Plenum Publishers, New York
3. Lehrer SS (1971) Solute perturbation of protein fluorescence. The quenching of the tryptophan fluorescence of model compounds and of lysozyme by iodide ion. Biochemistry 10:3254–3263
4. Lakowicz JR, Cherek H (1980) Nanosecond dipolar relaxation in proteins observed by wavelength-resolved lifetimes of tryptophan fluorescence. J Biol Chem 225:831–834
5. Lakowicz JR (2000) On spectral relaxation in proteins. Photochem Photobiol 72(4):421–437
6. Demchenko AP (2002) The red-edge effects: 30 years of exploration. Luminescence 17:19–42
7. Pan C-P, Barkley MD (2004) Conformational effects on tryptophan fluorescence in cyclic hexapeptides. Biophys J 86(6):3828–3835
8. Callis PR, Liu T (2004) Quantitative prediction of fluorescence quantum yield for tryptophan in proteins. J Phys Chem B 108:4248–4259
9. Hochstrasser RM, Negus DK (1984) Picosecond fluorescence decay of tryptophan in myoglobulin. Proc Natl Acad Sci 81:4399–4403
10. Chen Y, Barkley MD (1998) Toward understanding tryptophan fluorescence in proteins. Biochemistry 37:9976–9982
11. Kamal JKA, Behere DV (2001) Steady-state and picosecond time-resolved fluorescence studies on native and apo seed coat soybean peroxidase. Biochem Biophys Res Commun 289:427–433
12. Neves-Petersen MT, Gryczynski Z, Lakowicz J, Fojan P, Pedersen S, Petersen E, Petersen SB (2002) High probability of disrupting a disulphide bridge mediated by an endogenous excited tryptophan residue. Protein Sci 11:588–600
13. Carvalho ASL, Santos AM, Neves-Petersen MT, Petersen SB, Aires-Barros MR, Melo EP (2004) Conformational states of HRPA1 induced by thermal unfolding: Effect of low molecular weight solutes. Biopolymers 75:173–186
14. Prompers JJ, Hilbers CW, Pepermans HAM (1999) Tryptophan mediated photoreduction of disulphide bonds causes unusual fluorescence behaviour of *Fusarium solani pisi* cutinase. FEBS Lett 45(6):409–416
15. Bent DV, Hayon E (1975) Excited state chemistry of aromatic amino acids and related peptides. III. Tryptophan. J Am Chem Soc 97(10):2612–2619
16. Tsentalovich YP, Snytnokiva OA, Sagdeev RZ (2004) Properties of excited states of aqueous tryptophan. J Photochem Photobiol A: Chem 162:371–379
17. Neves-Petersen MT, Klitgaard S, Sundström V, Polívka T, Yartsev A, Pascher T, Petersen SB (2006) Photo-induced reaction dynamics in aromatic residues in proteins. Manuscript in preparation
18. Speiser S (1992) Molecular electronic energy transfer in bichromophoric molecules in solution and in a supersonic jet expansion. Pure Appl Chem 64(10):1481–1487
19. Selvin PR (2000) The renaissance of fluorescence energy transfer Nat Struct Biol 7(9):730–734
20. Scholes GD (2003) Long-range resonance energy transfer in molecular systems. Annu Rev Phys Chem 54:57–87
21. Davis LM, Parigger C (1992) Use of streak camera for time-resolved photon counting fluorimetry. Meas Sci Technol 3:85–90
22. Optronis.com, 2005 http://www.optronis.com/content/view/14/41/
23. Eaton DF (1990) Recommended methods for fluorescence decay analysis. Pure Appl Chem 62(8):1631–1648
24. Sau AK, Chen C-A, Cowan JA, Mazumdar S, Mitra S (2001) Steady-state and time-resolved fluorescence studies in wild type and mutant Chromatium vinosum high potential iron proteins: Holo- and apo-forms. Biophys J 81:2320–2330
25. Engelborghs Y (2001) The analysis of time resolved protein fluorescence in multi-tryptophan proteins. Spectrochim Acta Part A 57:2255–2270
26. Engelborghs Y (2003) Correlating protein structure and protein fluorescence. J Fluoresc 13(1):9–16
27. Hearn CH, Turcu E, Joens JA (1990) The near U.V. absorption of dimethyl sulfide, diethyl sulfide and dimethyl disulfide at $T = 300$ K. Atmos Env 24A(7):1939–1944
28. Smith AL (1996) Comparison of the ultraviolet absorption cross section of C_{60} buckminsterfullerene in the gas phase and in hexane solution. J Phys B: At Mol Opt Phys 29:4975–4980
29. Berman HM, Westbrook J, Feng Z, Gilliland G, Bhat TN, Weissig H, Shindyalov IN, Bourne PE (2000) The protein data bank. Nucl Acids Res 28:235–242.
30. Neves-Petersen MT, Jonson PH, Petersen SB (1999) Amino acid neighbours and detailed conformational analysis of cysteines in proteins. Protein Eng 12(7):535–548